

Comparing Galaxies and Ly α Absorbers at Low Redshift

Suzanne M. Linder

The Pennsylvania State University, University Park, PA 16802

ABSTRACT

A scenario is explored in which Ly α absorbers at low redshift arise from lines of sight through extended galaxy disks, including those of dwarf and low surface brightness galaxies. A population of galaxies is simulated based upon observed distributions of galaxy properties, and the gas disks are modeled using pressure and gravity confinement. Some parameter values are ruled out by comparing simulation results with the observed galaxy luminosity function, and constraints may be made on the absorbing cross sections of galaxies. Simulation results indicate that it is difficult to match absorbers with particular galaxies observationally since absorption typically occurs at high impact parameters (> 200 kpc) from luminous galaxies. Low impact parameter absorption is dominated by low luminosity dwarfs. A large fraction of absorption lines is found to originate from low surface brightness galaxies, so that the absorbing galaxy is likely to be misidentified. Low redshift Ly α absorber counts can easily be explained by moderately extended galaxy disks when low surface brightness galaxies are included, and it is easily possible to find a scenario which is consistent with observed the galaxy luminosity function, with low redshift Lyman limit absorber counts, and with standard nucleosynthesis predictions of the baryon density, Ω_B .

Subject headings: galaxies: fundamental parameters, luminosity function—intergalactic medium — quasars: absorption lines

1. Introduction

The numerous absorption lines seen shortward of hydrogen $\text{Ly}\alpha$ in quasar spectra are a powerful probe of gas in galaxies. Recent observations of the $\text{Ly}\alpha$ forest at low redshift (Bahcall et al. 1996) have allowed for studies which compare absorbers with nearby galaxies, but the nature of the lower column density $\text{Ly}\alpha$ absorbers remains controversial. Here I explore the possible connection of Lyman limit systems ($N_{\text{HI}} = 10^{17.2}$ to $10^{20.3} \text{ cm}^{-2}$) and $\text{Ly}\alpha$ forest absorbers ($N_{\text{HI}} < 10^{17.2} \text{ cm}^{-2}$) with galaxies at low redshifts by using simulations to relate properties of the galaxy population to absorbers. A complete understanding of galaxy formation and evolution will require knowledge of the properties of the low redshift galaxy population, including galaxies which are more difficult to detect. Absorbing galaxies should include dwarf and low surface brightness (LSB) galaxies. These objects are generally found to be rich in gas, so they must make at least some contribution to $\text{Ly}\alpha$ absorption. Numerous studies have found extended gaseous envelopes around dwarf galaxies, so that their absorbing cross sections might not be small as their name would imply.

Burbidge et al. (1977) first noted that known galaxies must have huge cross sections in order to explain the $\text{Ly}\alpha$ absorbers. However, galaxy disks may be quite extended when ionized gas is considered, and the absorption capabilities of the more recently discovered dwarf and LSB galaxies have not been explored. Recent studies have had some success in matching absorption lines with particular galaxies, although conclusions vary depending upon the column density threshold. Studies concentrating on high column density, low redshift absorbers generally find clear

associations with galaxies (Lanzetta et al. 1995a; Stocke et al. 1995; Steidel et al. 1997), while lower column density absorbers tend to be located far from any observed galaxy. Often one or more galaxies will be seen at several hundreds of kpc from the line of sight, so that it is unclear whether any of the galaxies are responsible for the absorption, although the absorbers are generally found to follow the large scale galaxy distribution (Le Brun, Bergeron, & Boissé 1996; Morris et al. 1993; Bowen, Blades, & Pettini 1996; Rauch, Weymann, & Morris 1996; Mo & Morris 1994; Salzer 1992; van Gorkom et al. 1996). A few absorbers have been found in cosmic voids (Stocke et al. 1995; Shull, Stocke, & Penton 1996), while limited attempts have been made to detect LSB galaxies near quasar lines of sight (van Gorkom et al. 1996). Several groups have tested for a physical connection between absorbers and galaxies by looking for an anticorrelation between the equivalent widths of the absorption lines and the impact parameters between the galaxies and lines of sight (Lanzetta et al. 1995a; Bowen et al. 1996; Le Brun et al. 1996). However, it is not possible to know that any particular absorption line has been matched to the correct galaxy, and some galaxies which are unidentified may be causing absorption. Thus it is also useful to estimate how many absorbers could arise from lines of sight through galaxies.

Many nearby galaxies have been discovered only recently due to a severe selection effect against LSB galaxies (Bothun, Impey & McGaugh 1997). Disney (1976) made the first quantitative analysis of this selection effect after realizing that galaxies obeying the Freeman (1970) law were within one magnitude of the typical night sky brightness. The primary goal of recent surveys for LSB galaxies has

been simply to obtain a representative sample of the nearby galaxy population (Schombert et al. 1992; Impey et al. 1996; Sprayberry et al. 1996; Dalcanton et al. 1997a; O’Neil, Bothun, & Cornell 1997). Most LSB galaxies exhibit a wide range of properties such as sizes and morphologies which are similar to those of high surface brightness (HSB) galaxies. The exceptions are Malin objects, which make up about 10% of the Schombert et al. (1992) catalog. These objects are highly extended and extremely low in surface brightness, and they are often among the most luminous galaxies known. While most surveys for LSB galaxies have been biased toward blue objects, varying colors have been observed by O’Neil et al. (1997). McGaugh (1996a) found that the distribution of central galaxy surface brightnesses is approximately flat to at least $\mu_0 = 24\ B\ \text{mag arcsec}^{-2}$. Evidence has been seen more recently for a falloff faintward of $24\ B\ \text{mag arcsec}^{-2}$ (O’Neil et al. 1997; Zwaan, Briggs, & Sprayberry 1997; Briggs 1997). O’Neil et al. (1997) attribute this effect to an inability of extremely low surface brightness galaxies to form in a cluster environment.

The gaseous extent of galaxies is highly uncertain. Several studies involving 21 cm mapping of galaxy disks have found ‘sharp edges,’ where the neutral hydrogen column density falls off quickly from a few times $10^{19}\ \text{cm}^{-2}$ to an undetectable level. Such ‘edges’ have been explained successfully by models where the ionization level increases rapidly from the optically thick to optically thin regime (Maloney 1993; Corbelli & Salpeter 1993; Dove & Shull 1994), thus making a sudden cutoff in the total column density of the gas unnecessary. A detection of ionized gas beyond the HI disk in NGC 253 has been made re-

cently (Bland-Hawthorn, Freeman, & Quinn 1997). Ionized outer disks could be quite extended if they are not severely affected by galaxy interactions. These extended structures may also be consistent with results of cosmological simulations, where galaxies form within extended sheets and filaments (Weinberg, Katz, & Hernquist 1997; Norman et al. 1997). Many absorbers are found to arise in the sheet structures which have already formed at high redshifts. Double line of sight observations (Dinshaw et al. 1994, 1995; Fang et al. 1996) have shown that absorbers are hundreds of kpc in size. Furthermore, these observations were found to be consistent with flattened absorbers having organized motion, such as rotating disks (Charlton, Churchill, & Linder 1995). Disks in reality are likely to be warped and broken, but when considering the average behavior of a large sample of galaxies, some systematic falloff in total column density with radius can be expected. Only field galaxies are considered here, without the effects of clustering and interactions.

The number density of galaxies at low redshift is also uncertain due to a possible abundance of LSB galaxies. An upper limit can be found by supposing that all absorbers are caused by galaxy disks. The average number of absorbers per unit redshift along a line of sight was found by Bahcall et al. (1996) to be $(dN/dz)_0 = 24.3 \pm 6.6$, complete to an equivalent width in $\text{Ly}\alpha$ of $0.24\ \text{\AA}$. The neutral hydrogen column density distribution is observed to be approximately a power law at high redshifts (but see Petitjean et al. (1993) and Charlton, Salpeter, & Linder (1994)) with a slope of -1.5. While an accurate distribution of neutral hydrogen column densities at low redshift has not been published yet, it is assumed to look similar to those at higher

redshifts. A significant change in slope is generally not observed between redshifts 4 and 2.7 for the column density range of interest here (Lu et al. 1996; Hu et al. 1995; Kirkman & Tytler 1997; Kim et al. 1997).

Section 2 of this paper describes the method, including defining and simulating galaxy populations and modeling the galaxy disks as absorbers. Results are discussed and compared with local luminosity functions, the predicted baryon density, and absorber/galaxy observations in section 3. Future papers will discuss the effects of clustering and the possibility of distinguishing between this scenario and others, such as those with significant nongalactic absorbers. The value of $H_0 = 100 \text{ km s}^{-1} \text{ Mpc}^{-1}$ is assumed.

2. Method

Samples of galaxies were simulated from a galaxy population as defined in section 2.1, where the method for choosing galaxy luminosities and surface brightnesses is explained. In each simulation, all of the galaxies were given random coordinates within a cube of space with a side length of 50 Mpc. Each galaxy disk was modeled using pressure and gravity confinement, as described in section 2.2. Lines of sight, going straight through the cube, were then chosen randomly. When a line of sight intersected a galaxy disk, the neutral column density was found by integrating the neutral gas density along the line of sight.

2.1. Defining a Galaxy Population

A galaxy population is defined here using simple parameter distributions which are consistent with observations. Galaxy luminosities are determined by the choice of scale lengths and central surface brightnesses. Re-

lations are then assumed between these observed parameters and the properties of the gas disks.

The surface brightness distribution is assumed to be flat with an exponential falloff at the high surface brightness (HSB) end, as in McGaugh (1996a). The LSB end is known to extend to at least $24 \text{ B mag arcsec}^{-2}$, while a few objects have been observed with $\mu_0 > 27 \text{ B mag arcsec}^{-2}$. Surface brightness profiles for the individual galaxy disks are assumed to be exponential, where the distribution of observed scale lengths is found to be a power law, $\phi(h_B) \propto h_B^n$, where $n \sim -2$ (van der Kruit 1987; Hudson & Lynden-Bell 1991; de Jong 1995). No correlation is assumed between scale length and central surface brightness, except that large, HSB objects are known not to exist (Sprayberry et al. 1995). Bothun, Impey & Malin (1991) have shown that the above distributions require a slope of -1.5 in the faint end of the galaxy luminosity function.

The bright end of the luminosity function is generally well fit by a Schechter function (Marzke, Huchra, & Geller 1994). Undiscovered Malin objects cause some incompleteness (McGaugh 1996a), although they are thought to be rare (Dalcanton, Spergel, & Summers 1997b; Hoffman, Silk, & Wyse 1992). Additional faint galaxies have been added in evolutionary models which avoid strong evolution in the faint blue galaxy population at higher redshifts (Gronwall & Koo 1995; McGaugh 1994; Driver et al. 1995). Sprayberry et al. (1997) found that a combined Schechter bright end and power law faint end ($M_B > -16$) provide the best fit for the observed luminosity function, including LSB galaxies, where the faint end slope was found to be quite steep (~ -2). Observed luminosity functions

(Driver & Phillips 1996; Zucca et al. 1996; Marzke et al. 1994) are generally found to be consistent with such hybrid shapes, including a Shechter function with $\alpha = -1$ and a power law with slope between -1.4 and -1.8 for $M_B > -16$, as discussed in Sprayberry et al. (1997). Here the disk scale length distribution, for a given μ_0 , obeys a power law if $M_B > M_{Bsw}$. For more luminous galaxies, a scale length is chosen, for a given central surface brightness, so that the Marzke et al. (1994) Shechter function is obeyed.

LSB galaxies obey the Tully-Fisher relation (Zwaan et al. 1995), and simulations by Navarro (1997) have hinted at a physical explanation for this relation. Here the Tully-Fisher formula from Jacoby et al. (1992) is used to determine a rotation velocity for each galaxy, which is needed to model the dark matter halo. Evidence is given by de Blok, McGaugh, & van der Hulst (1996) that LSB galaxies are low in central column density compared to HSB objects. A central column density value for HSB galaxies has been estimated by Bowen, Blades, & Pettini (1995). A relationship is assumed here which is consistent with the Bowen et al. (1995) estimate and which requires a factor of five change in surface brightness for a factor of two in central column density (McGaugh 1996b) so that the central column density becomes $N_0 = 10^{-0.17\mu_0 + 25.9} \text{ cm}^{-2}$.

2.2. Modeling Galaxy Disk Absorbers

The total (neutral plus ionized) column density is assumed to fall off exponentially in each inner disk and as a power law farther out:

$$N_{tot}(r) = \begin{cases} N_0 \exp(-r/h_{21}) & \text{for } r < r_{sw} \\ N_0 \exp(-r_{sw}/h_{21})(r/r_{sw})^{-p} & \text{for } r > r_{sw} \end{cases} \quad (1)$$

where r is the distance in the plane of the disk, r_{sw} is the value of r at which the switch from exponential to power law occurs, and h_{21} is an exponential scale length of the inner neutral hydrogen disk which could be determined using 21 cm mapping. Evidence for a power law falloff in outer galaxy disks has been seen by Hoffman et al. (1993), and such behavior is required for galaxies to produce a power law type neutral column density distribution. A neutral column density distribution which goes as $N_H^{-1.5}$ corresponds to $p = 4$. The value of r_{sw} is quite uncertain, and here it is assumed to be at one or two times the radius at which the gas becomes highly ionized (r_{cr}). The ratio of the neutral hydrogen scale length to B scale length (h_{21}/h_B) is also uncertain. An initial estimate of 3.4 is used here based upon the conjectures of Salpeter (1995), and a smaller value (1.7) is also tested.

The disks are modeled using pressure and gravity confinement (Charlton, Salpeter, & Hogan 1993; Charlton et al. 1994). The vertical structure is calculated in each disk, so that the internal pressure and density are related by $P(z, r) = 2n_{tot}(z, r)kT$, where the assumed temperature is $T = 20000 \text{ K}$, z is the height above the disk plane, and n_{tot} is the density of neutral plus ionized hydrogen. The inner disks are confined by a spherical dark halo with gravitational acceleration $g = V_{rot}^2 z/r^2$ where V_{rot} is the rotation velocity. The boundary condition $P(z = w/2) = P_{ext}$ defines the absorber width w . The outer disks are confined by an external pressure P_{ext} which may be due to infalling material or to a local or diffuse intergalactic medium. The high redshift value of $P_{ext}/k = 10 \text{ cm}^{-3} \text{ K}$

(Charlton et al. 1994) is used here, although more recently evidence has emerged supporting a similar value at low redshift (Wang & Ye 1997). Hydrostatic equilibrium is assumed, so that

$$\frac{dP}{dz} = -\frac{m_H P}{2kT} \frac{V_{rot}^2 z}{r^2} \quad (2)$$

where m_H is the mass of a hydrogen atom. The solution is

$$P(z) = P(0) \exp(z^2/h_z^2), \quad (3)$$

where

$$P(0) = P_{ext} \exp(w^2/4h_z^2), \quad (4)$$

is the pressure at $z = 0$, and

$$h_z = \frac{2r}{V_{rot}} \left(\frac{kT}{m_H} \right)^{1/2} \quad (5)$$

is the vertical scale height.

A model for the vertical ionization structure is used which is similar to that in Maloney (1993). The gas is assumed to be highly ionized above height z_i where

$$\int_{z_i}^{w/2} \alpha_{rec} n_{tot}^2(z) dz = \phi_{i,ex}, \quad (6)$$

and $\phi_{i,ex}$ is the ionizing flux, which has been measured at low redshift by Kulkarni & Fall (1993) using the proximity effect. The inner layer of gas below z_i is shielded and remains neutral. This sandwich structure occurs out to a fairly constant column density of about $3 \times 10^{19} \text{ cm}^{-2}$ for each galaxy. For $r > r_{cr}$, where the column density is below this critical value, ionization equilibrium is assumed, where $\alpha_{rec} n_{tot}^2 = \zeta n_H$ for neutral hydrogen density n_H , ζ is an average ionization rate, and $\alpha_{rec} = 4.07 \times 10^{13} \text{ cm}^3$

$\text{s}^{-1}(T/10,000\text{K})^{-0.75}$ is the recombination coefficient.

For lines of sight intersecting the inner disk, the observed column density is dominated by the neutral layer of gas, so that

$$N_{HI} = \frac{P(0)}{2kT} \int_{\text{los}} \exp(-z^2/h_z^2) dz \quad (7)$$

where the integral is performed along the line of sight (los) for $|z| < z_i$. For highly ionized gas ($r > r_{cr}$) the neutral column density becomes

$$N_{HI} = \frac{\alpha_{rec}}{\zeta} \frac{P(0)}{2kT} \int_{\text{los}} \exp(-2z^2/h_z^2) dz. \quad (8)$$

3. Results and Discussion

The first set of simulations each consisted of 20,000 lines of sight through a box containing 20,000 galaxies. The following standard parameters were used for each simulation, with the exceptions listed in Table 1.

- The slope of the neutral column density distribution was $\epsilon = 1.5$ (1.7 for run 1).
- The slope of the B scale length distribution was $n = -2$ (-1.35 for run 2).
- The cutoff in the surface brightness distribution was at $\mu_0 = 24 \text{ B mag arcsec}^{-2}$ (25 for run 3; 27 for run 9).
- The ionizing flux $\phi_{i,ex} = 4.6 \times 10^3 \text{ cm}^{-2}\text{s}^{-1}$ ($2.8 \times 10^4 \text{ cm}^{-2}\text{s}^{-1}$ for run 4).
- The ratio of the 21 cm scale length to B scale length was $h_{21}/h_B = 3.4$ (1.7 for run 5).
- The external pressure was $P_{ext}/k = 10 \text{ cm}^{-3} \text{ K}$ ($1 \text{ cm}^{-3} \text{ K}$ for run 6).

- The switch from exponential to power law falloff in total column density occurred at $r_{sw} = r_{cr}$ ($r_{sw} = 2r_{cr}$ for run 7).
- The luminosity function was changed from a Schechter form to a power law at $M_{Bsw} = -16$ (-15 for run 8).

3.1. Galaxy Counts and the Cosmological Density Parameter

The number density of galaxies for each simulation, listed in Table 1, is that which is required to explain the observed absorber counts of $(dN/dz)_0 = 24.3 \pm 6.6$ (Bahcall et al. 1996) for $N_{HI} > 10^{14.3} \text{ cm}^{-2}$. For galaxies with relatively large absorption cross sections (run 1) fewer galaxies are required, while the opposite effect is seen in runs 4, 5, 6, and 7. Since the central column density of the disk is assumed to vary rather weakly for a large change in surface brightness, LSB galaxies have bigger absorption cross sections at a given M_B compared to HSB galaxies, so that fewer galaxies are required if there are more LSB objects (runs 3 and 9). Absorption cross sections are generally found to increase with M_B , however, so that runs (2 and 8) where the shape of the luminosity function is changed to favor more luminous objects require fewer galaxies. Note that not all dwarf galaxies are required to be rich in gas as in these models, as the number density of galaxies is relatively insensitive to the faint end slope of the luminosity function. Some dwarfs may have formed recently or by varying mechanisms (Hunsberger, Charlton, & Zaritsky 1996).

The simulated luminosity functions (LFs), which are normalized to produce absorber counts, are shown in Figure 1. The Schechter function found by Marzke et al. (1994) and

the binned LF from Sprayberry et al. (1997) are also shown. The Marzke et al. (1994) function generally includes galaxies with $\mu_0 < 22 \text{ B mag arcsec}^{-2}$, while the Sprayberry et al. (1997) points are restricted to $\mu_0 > 22 \text{ B mag arcsec}^{-2}$, so that the sum of the two can be considered to be a fairly complete LF. Note that only models with relatively small galaxy absorption cross sections can provide a reasonable fit to the observed LF. In other words, models where galaxies have larger cross sections will overproduce dN/dz if they contain as many galaxies as are known to exist according to observed LFs. Therefore, by comparing with observed LFs, it is possible to rule out models with overly large galaxy cross sections, or put an upper limit on the characteristic size of absorbing galaxies. For example, a galaxy with $M_B^* = -18.9$ would have a radius of around 100-300 kpc in runs 4 and 5 down to a column density of $2 \times 10^{14} \text{ cm}^{-2}$, where some variations occur due to variations in central surface brightness. Smaller galaxy disks cannot be ruled out by this method, but then significant nongalactic absorption must also occur. Many parameter assumptions are also uncertain. For example, several galaxies with $\mu_0 \sim 27 \text{ B mag arcsec}^{-2}$ are known to exist, so there must be at least some tail at the LSB end of the surface brightness distribution. In reality, some adjustments or variations in all of the parameters are expected. It can be concluded, however, that it is easily possible to obtain a reasonable fit to the observed luminosity function, and thus explain absorbers using galaxies, within the range of parameter uncertainties.

A value for the cosmological density parameter Ω_{DM} , due to the given number density of galaxy halos required to match the observed $(dN/dz)_0$, is also shown in Table 1. It

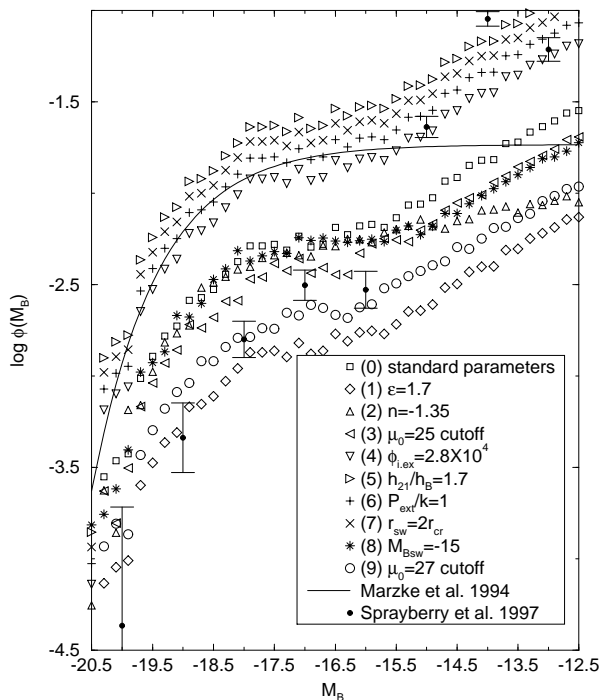


Fig. 1.— Simulated galaxy luminosity functions, which are normalized to produce observed absorber counts, are plotted along with observed LSB (binned points) and HSB (solid line) luminosity functions. Note that most of the runs shown here require fewer galaxies than are known to exist in order to explain the observed value of $(dN/dz)_0$.

is assumed that a flat rotation curve continues to three times the radius of the pressure-gravity confinement transition in each galaxy. Zaritsky et al. (1997) find that luminous spiral galaxy halos continue out to at least 200 kpc, which is consistent with the radius assumed for a typical L^* galaxy in run 4 or 5. The value of Ω_{DM} is generally found to be larger for models with a greater number density of required galaxies, although varying the shape of the faint end of the LF has little effect (runs 2 and 8). Simulations which produce enough galaxies compared to the ob-

served LF tend to have high values of Ω_{DM} . However, the value of Ω_{DM} is most sensitive to the shape of the bright end of the LF and the properties of the halos, which need to be modeled more accurately.

The value of Ω_B due to hydrogen in galaxies, which is also shown in Table 1, is more closely related to absorber counts. Here Ω_B is shown due to galaxies assuming each one cuts off at a neutral column density of $2 \times 10^{14} \text{ cm}^{-2}$, although varying the cutoff column density in each run has little effect. Assuming each galaxy has associated gas out to a column density of 10^{12} cm^{-2} increases Ω_B by less than $\sim 1\%$, while assuming that the gas cuts off at the pressure-gravity confinement transition decreases Ω_B by $< 10\%$. Previous estimates of Ω_B due to observed galaxies at low redshift have been much smaller than those from primordial nucleosynthesis predictions (Persic & Salucci 1992), but comparing with the value from Walker et al. (1991), $\Omega_B h_{100}^2 = 0.013 \pm 0.003$, most of the runs give baryon densities which are somewhat high. One exception is run 1, which also requires an unreasonably small number of galaxies as discussed above. Runs which give particularly high Ω_B include 4, 6 and 7. In run 4, a large amount of ionized gas is required, and in run 7, the gas is too highly concentrated in the centers of galaxies. In run 6, the disks must be confined by gravity out to larger radii, and a more rapid falloff in neutral column density occurs in the gravity dominated regime (Charlton et al. 1994), so again the gas is too centrally concentrated. It can be argued from the results of run 7 that galaxies must have surrounding gas which falls off slowly with radius (such as a power law rather than an exponential) in order for galaxies to explain most of the $\text{Ly}\alpha$ absorbers. The only remaining

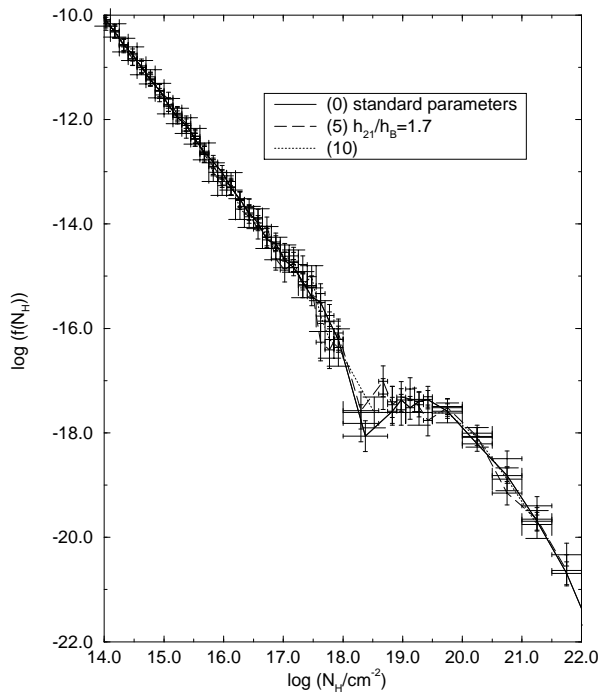


Fig. 2.— Simulated neutral column density distributions for low redshift $\text{Ly}\alpha$ absorption. Their shapes are determined primarily by the assumed slope, and therefore, and observed neutral column density distribution will be useful primarily for constraining this slope.

way to allow for a reasonable fit to the LF is to decrease the 21 cm scale lengths as in run 5, although the value of Ω_B remains slightly high.

It is possible that the amount of gas in galaxy centers has been overestimated by assuming exponential total column density profiles, since the observed central column densities tend to be about an order of magnitude smaller than the extrapolated fits to exponential profiles (Cayatte et al. 1994; de Blok et al. 1996). Most of this unobserved gas mass is likely to exist in the form of molecular gas or stars (McGaugh & de Blok 1997) so that Ω_B is not severely overestimated. A somewhat high

value of Ω_B obtained from the simple models used here cannot be taken too seriously for a given set of parameters, and small adjustments of multiple parameters can reduce the value of Ω_B . For example, adding more LSB galaxies would be reasonable, as some tail must exist at the LSB end of the surface brightness distribution, but the shape of this tail is highly uncertain. Also, decreasing r_{sw}/r_{cr} might make the models more realistic.

The number of Lyman limit absorbers is shown for each simulation in Table 1, again assuming that the total number of absorbers from Bahcall et al. (1996) is produced by galaxies. The number of Lyman limit absorbers has been measured at redshifts ≥ 0.36 , and the lowest redshift values available are within the range of $(dN/dz)_{LL} \sim 0.2$ to 1.3 (Lanzetta, Wolfe, & Turnshek 1995b; Storrie-Lombardi et al. 1994; Stengler-Larrea et al. 1995). Storrie-Lombardi et al. (1994) find a power law evolution in the number of Lyman limit systems which decreases at lower redshifts, while the Lanzetta et al. (1995b) and Stengler-Larrea et al. (1995) measurements are less sharply decreasing with redshift. Assuming that the evolution is flat or decreasing to $z \sim 0$, the values of $(dN/dz)_{0,LL}$ are slightly high for most runs. Runs 4, 6, and 7, which also had unreasonably high Ω_B , have excessive numbers of Lyman limit absorbers. Thus the same model parameters seem to be favored by comparing with Lyman limit absorber counts as with Ω_B , as discussed above.

Since there are likely to be small variations in all of the model parameters, no attempt is made to find a single best fitting set of parameters. Further discussions concentrate on the relatively reasonable run 10, which uses the standard parameters except for a surface brightness cutoff at 25 B mag arcsec $^{-2}$, a scale

length ratio of $h_{21}/h_B = 1.7$, and a change to a power law falloff in column density at $r_{sw} = 0.8r_{cr}$. In run 10, 20,000 galaxies and 30,000 lines of sight are simulated, and a number density of 2.0 galaxies Mpc^{-3} is required to explain absorber counts, giving $\Omega_{DM} = 0.37$, $\Omega_B = 0.017$, and $(dN/dz)_{0,LL} = 1.56$. Note that the Lyman limit systems are now produced in regions with power law falloffs in column density. The number of Lyman limit systems would be smaller if the column density profiles were modeled more realistically, so that the Lyman limit regime is produced in a region with column density falloff which is faster than the power law, yet slower than the exponential.

3.2. Implications for $\text{Ly}\alpha$ Absorbers

Simulated neutral column density distributions are shown in Figure 2 (for larger simulations consisting of 30,000 galaxies and 30,000 lines of sight in runs 0 and 5). Little variation is seen between different simulations since the normalization is fixed and the slope is not expected to vary much from -1.5 . A measurement of the observed slope at low redshift will be interesting, as the value of Ω_B is sensitive to small changes in ϵ , although constraints on the other model parameters are unlikely to be possible using an observed neutral column density distribution. A gap is seen in each simulation at $\sim 10^{19} \text{ cm}^{-2}$ due to the sudden increase in ionization, although it may be smoothed out in reality due to clumpiness in the gas or variations in the amount of ionizing radiation.

Absorption cross sections are found to increase with galaxy luminosity, as shown in Figure 3. Thus most absorbers will arise from luminous galaxies, although less luminous objects may produce some absorption

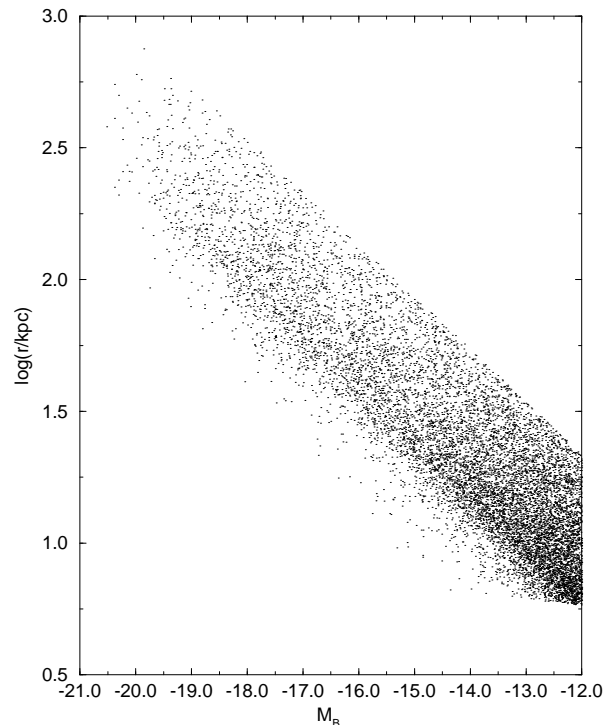


Fig. 3.— The absorbing ($> 2 \times 10^{14} \text{ cm}^{-2}$) radii of galaxies (simulated in run 10) increase with galaxy luminosity, although variation occurs at a given M_B which depends upon surface brightness.

since they are more numerous. It was also shown by Bowen et al. (1996) that absorption cross sections must depend upon galaxy luminosity. They argued that it is unlikely that low luminosity galaxies produce absorption due to this dependence, but a modest fraction of absorption at low impact parameters is produced by galaxies which are low in luminosity, as shown in Figures 4 and 5. Variations in surface brightness have less effect upon absorption cross section, but at a given M_B a lower surface brightness galaxy will be larger since the column density is assumed to vary weakly with surface brightness. Thus the upper points in Figure 3 show a sharp edge due to the unrealistic sharp cutoff assumed in

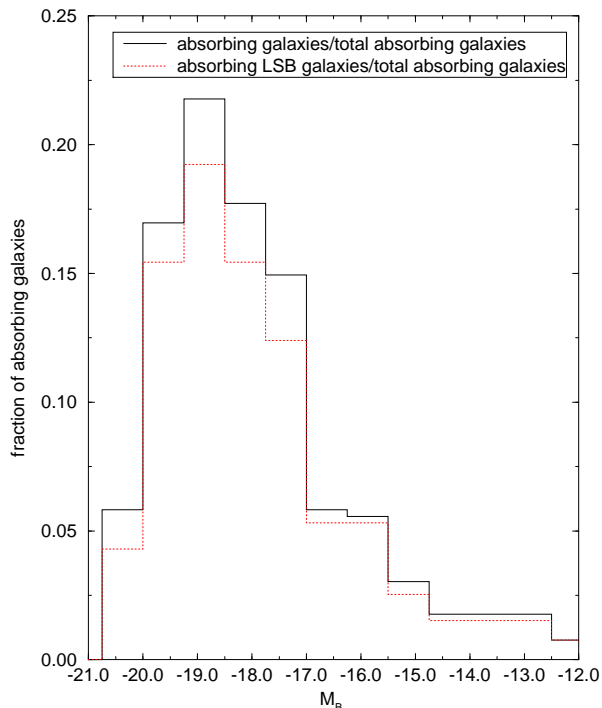


Fig. 4.— The fraction of absorbing ($> 10^{15} \text{ cm}^{-2}$) galaxies at impact parameters < 300 kpc is shown as a function of M_B for run 10. LSB galaxies, with $\mu_0 > 22 \text{ B mag arcsec}^{-2}$, may cause most of the $\text{Ly}\alpha$ absorption. Low luminosity dwarfs make a modest contribution to absorbing galaxies.

the surface brightness distribution, while the lower (HSB) points fall off more smoothly.

A surprisingly large fraction of absorbers ($> 10^{15} \text{ cm}^{-2}$) is shown to arise in LSB galaxies, as is seen in Figure 4. While this result is quite sensitive to the shape of the surface brightness distribution and to the relationship between column density and surface brightness, luminous HSB galaxies may make a relatively unimportant contribution to $\text{Ly}\alpha$ absorption. While LSB galaxies are thought to have relatively low central column densities, a strong correlation is not seen between column densities and surface brightnesses in de Blok

et al. (1996). Making this relationship weaker results in a larger contribution to absorption from LSB galaxies. In Figure 5, the absorbing ($> 10^{12} \text{ cm}^{-2}$) galaxy impact parameters are shown versus M_B . More luminous galaxies can absorb at larger impact parameters, as is consistent with Figure 3. It can also be seen that low luminosity galaxies make an important contribution to absorption if they are close to lines of sight and that a large fraction of absorbers arise in somewhat luminous LSB galaxies which allow for absorption at the largest impact parameters. Radio surveys for absorbing galaxies such as van Gorkom et al. (1996) find that absorbers include dwarf galaxies at relatively small impact parameters and luminous galaxies which are farther from lines of sight.

A plot of the galaxy impact parameters versus neutral column density is shown in Figure 6. While each galaxy is assumed to have a systematic falloff in column density with radius, a large amount of scatter is seen in the plot mostly due to variations in absorption cross sections of galaxies. Variations in disk inclinations contribute less to the scatter, so that any scenario in which absorption cross sections vary would produce a similar plot. However, when realistic selection effects are introduced, limiting the galaxy sample to a more narrow range of properties, less scatter is seen. A strong statistical anticorrelation is found for all (963) points simulated with $N_{HI} > 10^{14.3}$ using a Kendall rank correlation test. However, when random samples of 30 points are chosen, a $> 2\sigma$ anticorrelation is found in only 122 out of 200 samples. Furthermore, those samples which are strongly anticorrelated typically contain one high column density ($> 10^{20} \text{ cm}^{-2}$) system. Lanzetta et al. (1995a) observed an anticor-

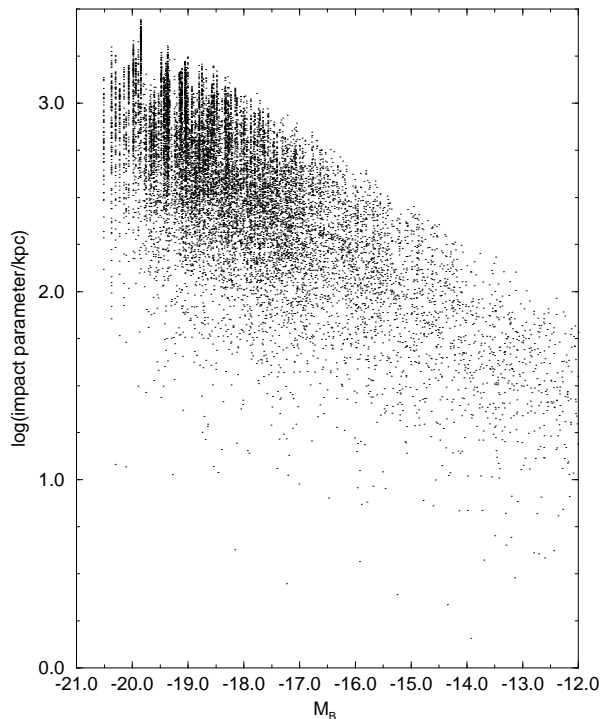


Fig. 5.— Impact parameters between lines of sight and absorbing ($> 10^{12} \text{ cm}^{-2}$) galaxies in run 10 versus M_B . Luminous galaxies can absorb out to larger impact parameters as is consistent with Figure 3. Note that most objects at low impact parameters are low in luminosity.

relation between equivalent width and corresponding galaxy impact parameter. Bowen et al. (1996) saw no obvious anticorrelation, which was used to argue that absorbers are more weakly associated with galaxies. Le Brun et al. (1996) observed luminous galaxies close to lines of sight, to a lower equivalent width limit. They found a weak anticorrelation between equivalent width and impact parameter. All of these results appear consistent with the scenario described here, and many more observations will be required to distinguish between absorber models.

The fraction of galaxies which cause ab-

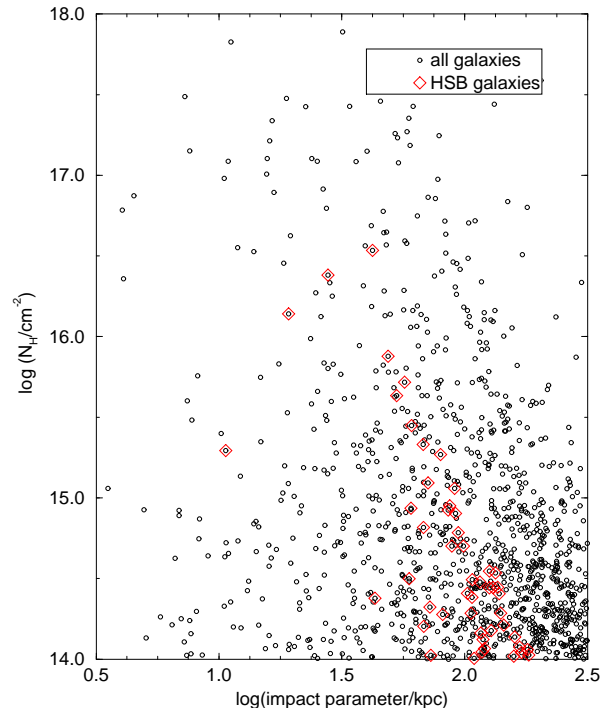


Fig. 6.— Impact parameters between absorbing galaxies and lines of sight in run 10 are plotted versus neutral column density for all galaxies (circles) and for HSB ($\mu_0 < 22 B \text{ mag arcsec}^{-2}$) galaxies (diamonds).

sorption is shown versus galaxy impact parameter in Figures 7a ($L > L^*$, $N_{\text{HI}} > 10^{14.3} \text{ cm}^{-2}$) and 7b ($L > 0.1L^*$, $N_{\text{HI}} > 10^{15} \text{ cm}^{-2}$). Bowen et al. (1996) find that their observed galaxies typically cause absorption out to 300 kpc, while Lanzetta et al. (1995a) find a smaller typical absorption cross section of about 160 kpc. This value is quite consistent with cross sections found for HSB, M_B^* galaxies. Lanzetta et al. (1995a) find that 5/5 galaxies with impact parameters < 70 kpc cause absorption, where these galaxies are slightly less luminous than the ones plotted in Figure 7a. Le Brun et al. (1996) find that all of 4 galaxies cause absorption within ~ 90 kpc where their selection effects are sim-

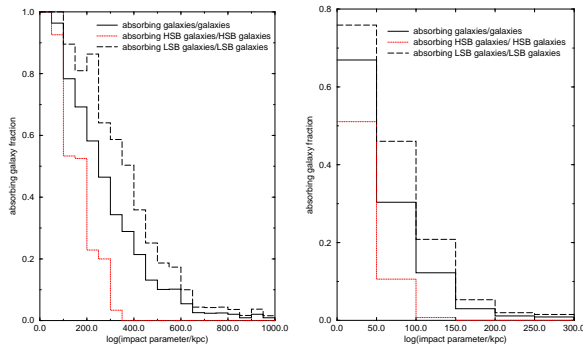


Fig. 7.— The covering factors, or fractions of galaxies causing absorption in a given impact parameter range are shown for run 10. The fraction of absorbing LSB ($\mu_0 > 22$ B mag arcsec $^{-2}$, dashed line) and HSB ($\mu_0 < 22$ B mag arcsec $^{-2}$, dotted line) galaxies in a given range of impact parameter which cause absorption are also shown separately. In Fig. 7a (7b) the plotted galaxies have luminosities $> L^*$ ($0.1L^*$) and cause absorption $> 10^{14.3}$ cm $^{-2}$ (10^{15} cm $^{-2}$). LSB galaxies are more likely to cause absorption as they have larger cross sections at a given luminosity.

ilar to those in Figure 7a. Bowen et al. (1996) find that 40 percent of galaxies cause absorption at impact parameters between 100 and 300 kpc, although their sample is not quite complete to $0.1L^*$ as in Figure 7b. While selection effects which depend upon redshift may explain some of the discrepancies, it is also likely that dwarf and LSB absorbers are being misidentified. In the simulation results here, the correct absorbing galaxy is known, while observers are likely to match an absorption line with the most easily visible galaxy.

The clustering properties of the galaxies would need to be included in the models in order to test whether galaxy misidentifications could help to explain the results from Bowen et al. (1996). LSB galaxies may be

weakly clustered around galaxies which are more easily seen, so that the absorption cross sections of some luminous galaxies may be overestimated. Many galaxies which are more difficult to detect may have formed within the same extended sheets which contain luminous, HSB galaxies as seen in cosmological simulations. It is also possible that a more clumpy distribution of gas around galaxies, such as that produced by tidal interactions (Morris & van den Bergh 1994), would be more realistic, although the covering factor of gas around the galaxies would need to remain high out to larger distances in order to be consistent with observations. Both Morris et al. (1993) and Le Brun et al. (1996) found that all luminous galaxies within 0.5 to 1 Mpc cause absorption with a lower equivalent width limit. It would be difficult to allow for individual galaxies having such large cross sections without overproducing absorber counts.

4. Conclusions

$\text{Ly}\alpha$ absorber counts at low redshift can easily be explained by lines of sight through moderately extended galaxy disks when low surface brightness galaxies are included. A scenario in which absorbers are explained by galaxies can easily be made consistent with observed luminosity functions, low redshift Lyman limit absorber counts, and predictions of Ω_B from standard nucleosynthesis. In successful models the absorption cross sections must increase with galaxy luminosity, where an L^* galaxy typically has an absorbing radius of ~ 200 kpc and a low luminosity dwarf has a radius ~ 10 kpc. Larger absorption cross sections are ruled out by observed luminosity functions, assuming that most galaxies are potential absorbers. The baryon density,

as predicted by primordial nucleosynthesis, is overproduced if the gas is too highly ionized or too concentrated in the centers of galaxies, while low surface brightness galaxies are less centrally concentrated, so that they can have larger absorption cross sections without containing excessive baryons.

Low surface brightness galaxies may make a large and important contribution to $\text{Ly}\alpha$ absorption. In fact, luminous, high surface brightness galaxies may make a relatively unimportant contribution. Luminous galaxies, especially those which are low in surface brightness, are responsible for most $\text{Ly}\alpha$ absorption lines, where the lower column densities are often due to luminous galaxies at large impact parameters. Low luminosity dwarfs are much more numerous, so that their contribution to absorption becomes more important when they are at smaller impact parameters from quasar lines of sight. Therefore, it may be generally difficult to observationally match a particular absorption line to the correct galaxy.

While a fairly small number of $\text{Ly}\alpha$ absorption lines have been matched to specific galaxies to date, these observations generally appear consistent with the scenario simulated here, given that it is impossible to know that any particular absorption line has been matched to the correct galaxy. A substantial fraction of $\text{Ly}\alpha$ absorption is likely to arise from lines of sight through low surface brightness galaxies which are clustered around more easily visible galaxies. These LSB galaxies are likely to be misidentified, and improved simulations which consider the clustering properties of these galaxies will be needed to quantify the effects of possible misidentifications. A much larger number of observations will be required to test possible models (Sarajedini,

Green, & Jannuzi 1996), and greater sensitivity to low surface brightness galaxies near quasar lines of sight will be required, even in places where luminous, high surface brightness galaxies have already been detected. Refinements to the models here which allow for reasonable clustering properties will allow for further constraints on the arrangement of neutral and ionized gas relative to galaxies in the nearby Universe.

I am grateful to J. Charlton, G. Bothun, C. Churchill, R. Ciardullo, S. McGaugh, J. Miralda-Escudé, and D. Schneider for valuable discussions and to D. Sprayberry for supplying data points. This work was supported by a fellowship from the NASA Graduate Student Researchers Program.

REFERENCES

- Bahcall, J. N., Bergeron, J., Boksenberg, A., Hartig, G. F., Jannuzi, B. T., Kirhakos, S., Sargent, W. L. W., Savage, B. D., Schneider, D. P., Turnshek, D. A., Weymann, R. J., & Wolfe, A. M. 1996, *ApJ*, 457, 19
- Bland-Hawthorn, J., Freeman, K. C., & Quinn, P. J. 1997, *ApJ*, in press
- Bothun, G. D., Impey, C., & McGaugh, S. 1997, *PASP*, 110, 745
- Bothun, G. D., Impey, C., & Malin, D. F. 1991, *ApJ*, 376, 404
- Bowen, D. V., Blades, J. C., & Pettini, M. 1996, *ApJ*, 464, 141
- Bowen, D. V., Blades, J. C., & Pettini, M. 1995, *ApJ*, 448, 662
- Burbidge, G., O'Dell, S. L., Roberts, D. H., & Smith, H. E. 1977, *ApJ*, 218, 33
- Briggs, F. H. 1997, *ApJ*, 484, 618
- Cayatte, V., Kotanyi, C., Balkowski, C., & van Gorkom, J. H. 1994, *AJ*, 107, 1003
- Charlton, J. C., Churchill, C. W., & Linder, S. M. 1995, *ApJ*, 452, L81
- Charlton, J. C., Salpeter, E. E., & Linder, S. M. 1994, *ApJ*, 430, L29
- Charlton, J. C., Salpeter, E. E., & Hogan, C. J. 1993, *ApJ*, 402, 493

- Corbelli, E. & Salpeter, E. E. 1993, *ApJ*, 419, 104
- Dalcanton, J. J., Spergel, D. N., Gunn, J. E., Schneider, D. P., & Schmidt, M. 1997, *AJ*, 114, 635
- Dalcanton, J. J., Spergel, D. N., & Summers, F. J., 1997a *ApJ*, 482, 659
- de Blok, W. J. G., McGaugh, S. S., & van der Hulst, J. M. 1996, *MNRAS*, 283, 18
- de Jong, R. S. 1995, PhD thesis, University of Groningen
- de Jong, R. S., & van der Kruit, P. C. 1994, *A&A*, 106, S451
- Dinshaw, N., Foltz, C. B., Impey, C. D., Weymann, R. J., & Morris, S. L. 1995, *Nature*, 373, 223
- Dinshaw, N., Impey, C. D., Foltz, C. B., Weymann, R. J., & Chaffee, F. H. 1994, *ApJ*, 437, L87
- Disney, M. J., 1976, *Nature*, 263, 573
- Dove, J. B. & Shull, J. M. 1994, *ApJ*, 423, 196
- Driver, S. P. & Phillipps, S. 1996, *ApJ*, 469, 529
- Driver, S. P., Windhorst, R. A., Ostrander, E. J., Keel, W. C., Griffiths, R. E., & Ratnatunga, K. U. 1995, *ApJ*, 449, L23
- Freeman, K. C. 1970, *ApJ*, 160, 811
- Fang, Y., Duncan, R. C., Crotts, A. P. S., & Bechtold, J. 1996, *ApJ*, 462, 77
- Gronwall, C. & Koo, D. C. 1995, *ApJ*, 440, L1
- Hoffman, G. L., Lu, N. Y., Salpeter, E. E., Farhat, B., Lamphier, B., & Roos, T. 1993, *AJ*, 106, 39
- Hoffman, Y., Silk, J., & Wyse, R. F. G. 1992, *ApJ*, 388, L13
- Hu, E. M., Kim, T.-S., Cowie, L. L., Songalia, A., & Rauch, M. 1995, *AJ*, 110, 1526
- Hudson, M. J. & Lynden-Bell, D. 1991, *MNRAS*, 252, 219
- Hunsberger, S. D., Charlton, J. C., & Zaritsky, D. 1996, *ApJ*, 462, 50
- Impey, C., Sprayberry, D., Irwin, M., & Bothun, G. 1996, *ApJ*, 105, S209
- Jacoby, G. H., Branch, D., Ciardullo, R., Davies, R. L., Harris, W. E., Pierce, M. J., Pritchet, C. J., Tonry, J. L., & Welch, D. L. 1992, *PASP*, 104, 599
- Kim, T.-S., Hu, E. M., Cowie, L. M., & Songalia, A. 1997, *AJ*, 114, 1
- Kirkman, D. & Tytler, D. 1997, *ApJ*, 484, 672
- Kulkarni, V. P., & Fall, S. M. 1993, *ApJ*, 413, L63
- Lanzetta, K. M., Bowen, D. V., Tytler, D., & Webb, J. K. 1995a, *ApJ*, 442, 538
- Lanzetta, K. M., Wolfe, A. M., & Turnshek, D. A. 1995b, *ApJ*, 440, 435
- Le Brun, V., Bergeron, J., & Boissé, P. 1996, *A&A*, 306, L691
- Lu, L., Sargent, W. L. W., Womble, D. S., & Takada-Hidai, M. 1996 *ApJ*, 472, L509
- Maloney, P. 1993, *ApJ*, 414, 41
- Marzke, R. O., Huchra, J. P., & Geller, M. J. 1994, *ApJ*, 428, 43
- McGaugh, S. S. & de Blok, W. J. G. 1997, *ApJ*, 481, 689
- McGaugh, S. S. 1996a, *MNRAS*, 280, 337
- McGaugh, S. S. 1996b, in *New Light on Galaxy Evolution*, IAU Symposium 171, eds. Bender, R. & Davies, R. L.
- McGaugh, S. S. 1994, *Nature*, 367, 538
- Mo, H. J. & Morris, S. L. 1994, *MNRAS*, 269, 52
- Morris, S. L. & van den Bergh, S. 1994, *ApJ*, 427, 696
- Morris, S. L., Weymann, R. J., Dressler, A., McCarthy, P. J., Smith, B. A., Terriale, R. J., Giovanelli, R., & Irwin, M. 1993, *ApJ*, 419, 524
- Navarro, J. F. 1997, preprint
- Norman, M. L., Zhang, Y., Anninos, P., & Meiksin, A. 1997, *ApJ*, in press
- O'Neil, K., Bothun, G. D., & Cornell, M., 1997, *AJ*, 113, 1212
- Persic, M. & Salucci, P. 1992, *MNRAS*, 258, P14
- Petitjean, P., Webb, J. K., Rauch, M., Carswell, R. F., & Lanzetta, K. 1993, *MNRAS*, 262, 499
- Rauch, M., Weymann, R. J., & Morris, S. L. 1996, *ApJ*, 458, 518
- Salpeter, E. E. 1995, in *The Physics of the Interstellar Medium and the Intergalactic Medium*, ASP Conference Series, vol. 80
- Salzer, J. J. 1992, *AJ*, 103, 385
- Sarajedini, V. L., Green, R. F., & Jannuzi, B. T. 1996, *ApJ*, 457, S542
- Schombert, J. M., Bothun, G. D., Schneider, S. E., & McGaugh, S. S., 1992, *AJ*, 103, 1107
- Shull, J. M., Stocke, J. T., & Penton, S. 1996, *AJ*, 111, 72
- Sprayberry, D., Impey, C. D., Irwin, M. J., & Bothun, G. D. 1997, *ApJ*, 482, 104
- Sprayberry, D., Impey, C. D., & Irwin, M. J. 1996, *ApJ*, 463, 535
- Sprayberry, D., Impey, C. D., Bothun, G. D., & Irwin, M. J. 1995, *AJ*, 109, 558
- Steidel, C. C., Dickinson, M., Meyer, D. M., Adelberger, K. L., & Sembach, K. R. 1997, *ApJ*, 480, S568
- Stengler-Larrea, E. A., Boksenberg, A., Steidel, C. C., Sargent, W. L. W., Bahcall, J. N., Bergeron, J., Hartig, G. F., Jannuzi, B. T., Kirhakos, S., Savage, B. D., Schneider, D. P., Turnshek, D. A., &

- Weymann, R. J. 1995, *ApJ*, 444, 64
- Stocke, J. T., Shull, J. M., Penton, S., Donahue, M., & Carilli, C. 1995, *ApJ*, 451, 24
- Storrie-Lombardi, L. J., McMahon, R. G., Irwin, M. J., & Hazard, C. 1994, *ApJ*, 427, L13
- van der Kruit, P. C., 1987, *A&A*, 173, 59
- van Gorkom, J. H., Carilli, C. L., Stocke, J. T., Perlman, E. S. & Shull, J. M. 1996, *AJ*, 112, 1397
- Walker, T. P., Steigman, G., Schramm, D. N., Olive, K. A., & Kang, H.-S. 1991, *ApJ*, 376, 51
- Wang, Q. D. & Ye, T. 1996, *New Astr.*, 1, 245
- Weinberg, D. H., Katz, N., & Hernquist, L. 1997 in *Origins*, eds. J. M. Shull, C. E. Woodard & H. Thronson (ASP Conference Series)
- Zaritsky, D., Smith, R., Frenk, C., & White, S. D. M. 1997, *ApJ*, 478, 39
- Zucca, E. et al. 1996, in 37th Herstmonceaux Conference, *HST and The High Redshift Universe*, ed. M. Pettini, (Cambridge: Cambridge University Press)
- Zwaan, M. A., Briggs, F., & Sprayberry, D. 1997, preprint
- Zwaan, M. A., van der Hulst, J. M., de Blok, W. J. G., & McGaugh, S. S. 1995, *MNRAS*, 273, L35

TABLE 1
SIMULATION RESULTS

run #	parameters varied	galaxies $(\text{Mpc})^{-3}$	Ω_{DM}	Ω_B	$(dN/dz)_{0,LL}$
0	all standard	0.62	0.21	0.021	1.59
1	$\epsilon = 1.7$	0.16	0.06	0.006	0.415
2	$n = -1.35$	0.28	0.19	0.020	1.39
3	$\mu_0 = 25$ cutoff	0.52	0.16	0.018	1.31
4	$\phi_{i,ex} = 2.8 \times 10^4$	1.4	0.50	0.049	2.25
5	$h_{21}/h_B = 1.7$	2.8	0.53	0.023	1.41
6	$P_{ext}/k = 1$	1.9	1.00	0.063	4.77
7	$r_{sw} = 2r_{cr}$	2.3	0.44	0.077	4.04
8	$M_{Bsw} = -15$	0.44	0.21	0.021	1.34
9	$\mu_0 = 27$ cutoff	0.39	0.11	0.014	1.22

NOTE.—Columns are: (3) the number density of galaxies required to explain absorber counts, (4) the cosmological density parameter due to dark matter halos (out to three times the gravity confinement radius in each galaxy), (5) the cosmological density parameter due to hydrogen (out to a column density of $10^{14.3} \text{ cm}^{-2}$), and (6) the number of Lyman limit systems per unit redshift.